A comparison of statistical and deterministic methods for shallow landslide susceptibility zoning in clayey soils

Authors: Ciurleo M., Cascini L., Calvello M.

ABSTRACT

Shallow landslides are widespread in different geological contexts and generally occur as multiple events over large areas. When these phenomena involve fine-grained soils, they may cause serious consequences—in terms of environmental and property damages—and thus their spatial forecasting becomes a relevant issue for land use planning and design purposes. The existing literature provides several methods for landslide susceptibility assessment, categorized in qualitative and quantitative methods. When dealing with analyses at large scale (1:5000), quantitative methods are generally preferred. In this paper, landslide susceptibility maps are produced for a study area prone to shallow landsliding, located in Catanzaro (southern Italy). To this aim, two quantitative methods are implemented: the statistical "information value method" and the deterministic "TRIGRS model." The two approaches are compared by means of two indicators of the grade of correctness of the landslide susceptibility maps: the area under curve of the ROC curve, AUC, and the overestimation index, OI. The results of the analyses in terms of AUC values demonstrate the effectiveness and consistency of both methods in performing the susceptibility mapping of the study area. When the OI values are considered, the results provided by the deterministic model are slightly better than the ones resulting from the statistical analysis. This does not come as a surprise for the case study at hand and it can be ascribed to the availability, within the study area, of: a reliable database of soil properties, and an in-depth knowledge of the behaviour of the considered landslides.

Keywords: fine-grained soils, shallow landslides, susceptibility, zoning, statistical analysis, deterministic analysis, comparison

Highlights

- Susceptibility zoning for shallow landslides in fine-grained soils at large scale
- Statistical and deterministic methods applied to a study area in Italy
- Comparison of zoning maps from statistical and deterministic analyses
- Proven effectiveness of both analyses for susceptibility zoning at large scale

1. Introduction

Rainfall-induced shallow landslides are widespread all over the world and, during a single rainfall event, they can involve large areas (Park et al., 2013; Lee and Park, 2016; Romer and Ferentinou, 2016; among others). The consequences caused by these phenomena are linked to a series of factors, among which: the geological context of the area affected by landsliding, the mechanical characteristics of the soils, the vulnerability of the exposed elements.

Shallow landslides of flow type in coarse-grained soils are generally characterized by both scarcity of warning signs in the pre-failure stage and high velocities in the post-failure phase (McDougall and Hungr, 2004; Sorbino et al., 2010; Hungr et al. 2014; Yerro et al., 2016). On the other hand, shallow landslides involving clayey colluvial soils frequently present warning signs in the pre-failure stage (e.g., tension cracks at the top of the slope) and a shorter run-out in the post failure phase (Hungr et al. 2001; Meisina et al., 2006; Cascini et al., 2015). Many examples of rainfall-induced shallow landslides in both coarse-grained and fine-grained soils are reported in Europe (e.g., Borrelli et al., 2012; Martinović et al., 2016), America (e.g., Baum et al., 2005; Godt et al., 2008), Asia (e.g., Park et al., 2013; Hadmoko et al., 2017) and Africa (e.g., Broothaerts et al., 2012; Romer and Ferentinou, 2016). A significant number of contributions specifically deal with the assessment of shallow landslide susceptibility (e.g., Leventhal and Kotze, 2008; Nandi and Shakoor, 2009; Frattini et al., 2010; Kavzoglu et al., 2015; Romer and Ferentinou, 2016).

Landslide susceptibility assessment, herein intended as the landslide spatial probability of occurrence within a given territory, can be performed by qualitative or quantitative methods, depending on how the landslide causal factors are considered and modelled (Lee and Park, 2016). The applicability of each method depends on: the availability, quality and accuracy of the data; the resolution of zoning; the required outcomes; and the scale of analysis (Soeters and van Westen, 1996; Cascini, 2008; Fell et al., 2008). Quantitative analyses can be divided into statistical and deterministic methods (Soeters and van Westen, 1996). Statistical methods, applicable at different scales (from 1:100,000 to 1:5000), establish the relationships between predisposing factors and landslides through the proper use of statistic indicators (Carrara, 1983; Baeza and Corominas, 2001; Nefeslioglu et al. 2008), while neglecting to explicitly model the landslide failure mechanisms (Park et al., 2013). Deterministic methods, applicable at large and detailed scales (≥1:5000), properly analyze existing or potential failure mechanisms via physically-based models calibrated using on-site and laboratory test results (Salciarini et al., 2006; Huang and Kao 2006; Godt et al., 2008; Park et al., 2013).

Several significant examples of the application of landslide statistical analyses at large scale are available in the literature (Cervi et al., 2010; Reza and Daneshvar, 2014; Iovine et al., 2014; Regmi et al., 2014). In some cases, a separation between different types of landslides is lacking and, for instance, slides, creep phenomena and falls may be considered together when deriving the event map for the statistical correlations (Hadmoko et al., 2017). On the other hand, a proper understanding of the landslide triggering processes is typically a key prerequisite for a consistent application of physically based models estimating shallow rainfall-triggered landslide susceptibility (Godt et al., 2008; Sorbino et al., 2010; Cascini et al., 2017). Only few contributions deal with the comparison between the results of statistical and deterministic methods applied to the same study area at large scale (Cervi et al. 2010; Armas et al., 2013).

Starting from the abovementioned aspects, the paper highlights the important role played by the understanding of the landslide mechanisms for the susceptibility assessment of shallow landslides in clayey soils. This aim is pursued by means of a skilled application of both statistical and deterministic methods in a study area located in southern Italy. The issue is dealt with at large scale (1:5000) thus allowing a thorough study of all the factors playing a significant role during the pre-failure and failure stages of landsliding. Particularly, the paper preliminary focuses on the characteristics of the analysed phenomena, then performs a susceptibility assessment of the study area by means of the statistical method known as "information value" (e.g. Yin and Yan, 1988) and of the physically-based model "TRIGRS" (e.g. Montgomery and Dietrich, 1994). Both methods end with the production of landslide susceptibility computational maps. The maps are compared and critically analysed in order to highlight advantages and limitations related to the two different methods of analysis.

2. Materials and Method

2.1. Study area and data set

The study area is located in southern Italy, in the Calabria region, within a larger area of 136 Km^2 (Fig. 1) that has been frequently affected by landslides (Antronico et al., 2013; Borrelli et al., 2015; Gullà et al., 2004, 2008; Cascini et al., 2015; Ciurleo et al., 2016). In this area, more than 60% of not flat land (i.e. slope angle greater than 5°) is covered by Pliocene light blue-grey silty clays. In this area two sites, indicated in the Figure as S2 and S3, have been already analysed by Gullà et al. (2004), Cascini et al. (2015) and Cascini et al. (2017). The focus of the present paper is the site, indicated in the Figure as S1, already partly analysed by Cascini et al. (2015) and Calvello and

Ciurleo (2016). The chosen site of interest is deemed to be the most representative in relation to two important shallow landslide events, which respectively occurred in 2009 and 2010.

The homogeneity of the fine-grained soils outcropping in the sites S1, S2 and S3 emerges from a comparison of geotechnical properties (Fig. 2). In the entire area, the soils can be classified as inorganic, inactive clays characterized by high plasticity and a high liquid limit (Fig. 2b). All the grain size distribution data fall within a well-defined grain size envelope; the upper limit shows a fine-grained fraction ranging from 89% to 99%, while the amount of sand varies from 1% to 11%. The index properties of the soil, the minimum and maximum values assumed by the void ratio and the soil porosity are summarized in Fig. 2b. The available shear strength envelope ranges from an upper limit, with a cohesion value of 24.3 kPa and a friction angle of 35.2°, to a lower limit characterized by a cohesion value of 2 kPa and a friction angle of 22.3°. The saturated permeability (Ks) ranges from 3.1×10^{-8} m/s to 7.65×10^{-7} m/s (Gullà et al., 2004, 2008; Cascini et al., 2015), reaching a value of $5x10^{-6}$ m/s in the topmost cracked weathered layers (Cascini et al., 2017).

Owing to the homogeneity of the geotechnical data, the information gathered by previous studies in the sites S2 and S3 have been combined with those available in the study areas, i.e. site S1. The study area is located on the left bank of the Corace river, it covers approximately 8 km^2 and it represents the product of a complex geological evolutive model provided by Cascini et al. (2015). The topographical and morphological data used for the analyses are derived from a digital elevation model with a 5 m resolution generated from digital topographic maps of the Calabria Region (1:5000 scale, year 2005). The available geological information, provided in Fig. 3, shows that the outcropping lithology is mainly characterized by silty clays, partially affected by intercalations of sands. A sandstone layer constituting a morphoselective scarp, which is about 10 to 30 m thick and covers 2.5% of the test site, will not be included in the analysis, given the study focuses on shallow landslide susceptibility in fine-grained soils.

The fine-grained soils, outcropping in S1 and in nearby areas, are involved in several processes that can be considered landslide predisposing factors (e.g., weathering of the most shallow layers, formation of cracks). The combination of these factors leads to an evolutionary pattern of the landslides lasting few years, from the first warning signs in the pre-failure stage to the end of movements (Fig. 4). It follows that the landslide inventory map has to be continuously updated. As reported in Fig. 5a, the original landslide inventory in the study area is dated 2009 and was updated in 2010.

Using aerial photos and satellite images from Google Earth, 117 and 509 shallow landslide triggering areas of slide type were inventoried in 2009 and in 2010, respectively. It is worth

130 highlighting that in 2009 the total area affected by landslides is equal to 0.09 Km^2, while in 2010
131 this area is about 0.2 Km^2. The smallest triggering landslide area is about 9 m^2 while the largest one
132 is 6000 m^2; the depths of the slip surfaces range from few decimetres to 3 meters. Considering that
133 the sliding surfaces' depths depend on their location on the slope, Cascini et al. (2017) proposed a
134 methodology to map the thickness of degraded rock. The methodology, which was initially
135 calibrated and validated by the authors over one morphological hollow (0.3 km^2 size), is herein
136 applied to map the weathered thickness for the entire study area (Fig. 5b). Fig. 5b underlines the
137 presence of low values of thickness on sharply defined ridges (up to 0.5 m) and at the top of the
138 slopes (from 0.5 m to 1.5 m) and maximum thickness depths higher than 5m at the valley bottom.
139 Significant phases of the morphological slope evolution due to shallow landslides are generally
140 related to short and intense rainfall events. The analysis of the rainfall patterns in relation to the
141 activity of the considered landslides is beyond the scope of the present paper yet it's worth
142 highlighting, herein, some findings on "critical rainfall" conditions for the area coming from
143 previous works (Gullà et al., 2004; Cascini et al., 2017). Referring to shallow landslides that
144 respectively occurred in site S2, in 2002 and 2003, and in Site S1, in 2009, these studies indicated
145 the maximum intensity of the rainfall event ranging from 43 mm (2002-2003) to 70 mm (2009) over
146 2 consecutive days and equal to 162 mm over six consecutive days (2009).
147
148 ## 2.2 Methods

149 The methodology used herein to assess the susceptibility to shallow landslides in fine-grained soils
150 starts with the calibration of the statistical and physically-based models and it ends with the
151 production of landslide susceptibility computational maps by means of both statistical and
152 deterministic methods. Both maps are computed and plotted using terrain computational units,
153 TCUs (Calvello et al., 2013), and discretizing the study area by means of square cells whose
154 dimension (herein 5 m by 5 m) is related to the employed scale of the analysis (1:5000 scale).
155 The statistical analyses are based on bivariate correlations (Tangestani, 2009; Conforti et al., 2012;
156 Ciurleo et al., 2016) over the study area, between available independent variables (e.g. elevation
157 zone, slope gradient, slope curvature) and a dichotomous dependent variable derived from the
158 available landslide inventories. The independent variables can be either categorical or numerical.
159 The categorical variables are divided in a number of classes directly correlated to the subdivision in
160 classes of the thematic maps from which they are derived; the numerical variables are herein always
161 divided in eight classes using the the Jenks Natural Breaks algorithm (Jenks, 1977). Following this

classification method, class breaks are identified as the boundaries that best group similar values and that maximize the differences between classes.

The dependent variables used for the analyses are the two already-mentioned landslide inventories dated 2009 and 2010. For both landslide inventories, the statistical weight assigned to each class, j, of each variable, Vi, is computed using the following formula, originally proposed within the "information value method" (e.g. Yin and Yan, 1988):

$$W_{ij} = log\left(\frac{D_{ij}}{D^*}\right) = log(\frac{F_{ij}/N_{ij}}{F_{tot}/N_{tot}}) \quad (1)$$

where: W_{ij} is the weight assigned to the class j of the independent variable Vi; D_{ij} is the density of landslides within class j of the independent variable Vi; D^* is the average density of landslides within the study area; F_{ij} is the number of TCUs with landslides belonging to the class j of the independent variable Vi; N_{ij} is the number of TCUs belonging to the class j of the independent variable Vi; F_{tot} is the total number of TCUs with landslides within the study area; N_{tot} is the total number of TCUs within the study area.

When W_{ij} assumes low negative value, the statistical implication is low probability for TCUs belonging to a given class of a given variable to be affected by landslides; when W_{ij} assumes high positive values, there's a high probability that TCUs belonging to that class are affected by landslides. When landslides are not present in a given class of a given independent variable, Eq. 1 cannot be used to compute the weight values. In such cases, the class weight is herein set to a value equal to the closest negative integer inferior to the minimum computed weight for all classes of all variables (Ciurleo et al., 2016).

The performance assessment of the bivariate correlation between the independent and the dependent variables used herein is based on the criteria proposed by Ciurleo et al. (2016), which employ two indicators, β and σ, defined as follows:

$$\beta_i = \frac{TPR_i}{FPR_i} = \frac{Sensitivity_{\ i}}{1-Specificity_{\ i}} \quad (2)$$

$$\sigma_i = \sqrt{\frac{\sum_{j=1}^{n}\left(W_{ij}^* - \underline{W}_i\right)^2}{n-1}} \quad (3)$$

where: TPR_i is the true positive rate (sensitivity of the bivariate model) for the independent variable Vi; FPR_i is the false positive rate for the independent variable Vi (1- specificity of the bivariate model); W_{ij}^* is the normalized value of the weight assigned to the class j of the independent variable Vi (Ciurleo et al., 2016); W_i is the average value of the weights assigned to the classes of the independent variable Vi; n is the number of classes of the independent variable Vi.

The two indicators computed with Eqs. (2) and (3) have been originally proposed to select the independent variables that are relevant for a statistical analysis based on bivariate correlations between them and one dependent variable. Herein they will be used to verify that all the considered variables are significant for the performed analysis.

Finally, the calibrated computational map is evaluated by means of a multivariate computational susceptibility index, IS_{TCU}, which is assigned to each TCU according to the following formula:

$$IS_{TCU} = \sum_i W_{ik(i)} \quad (4)$$

where: $W_{ik(i)}$ is the weight index of the relevant independent variable Vi related to the TCU belonging to class k(i) of that variable.

The deterministic analyses are based on TRIGRS (Montgomery and Dietrich, 1994), a physically-based model that is widely used for determining the distribution of shallow precipitation-induced landslide source areas in different geological contexts (Godt et al., 2008; Montrasio et al., 2011; Sorbino et al., 2010). The analysis couples a hydrologic model with an infinite slope stability computation in order to analyze the pore water pressure regime and then evaluate a distribution of factors of safety (FS) over large areas. In particular, TRIGRS models rainfall infiltration by solving the Richards equation for vertical infiltration that may occur during a precipitation event (Srivastava and Yeh, 1991) in homogeneous isotropic materials. It analyzes the slope stability using a simple infinite-slope analysis (Taylor, 1948) to compute FS for each cell of the computational domain. TRIGRS, used in conjunction with geographic information system (GIS) software, allows to obtain maps of FS results thus allowing to differentiate stable (FS>1) from unstable cells (FS≤1). Among the disadvantages of TRIGRS, it is worth listing the following: steady or quasi-steady models are not applicable to several realistic cases (e.g. Wu and Sidle, 1995; Sorbino et al., 2010); the model needs abundant and accurate spatial information over large portions of the study area in order to obtain reliable results; the results are quite sensitive to some of the input data, such as topographic data (slope gradient), hydraulic properties of soils (saturated vertical hydraulic conductivity, hydraulic diffusivity, saturated and residual volumetric water contents), initial water-table and soil

depths (Sorbino et al., 2010). Other input data the model needs are: rainfall data (with durations ranging from hours to a few days), cohesion, friction angle and total unit weight of soils. To sum up, realistic results from deterministic analyses based on TRIGRS are strictly linked to: a consistent identification of the in situ pore pressure regime, a good knowledge of mechanical and hydraulic soil properties, an accurate weathered thickness map, and a deep understanding of the triggering mechanisms of the considered landslides. The sensitivity of TRIGRS to soil thickness has been tested in Cascini et al. (2017). In the present paper we will test its sensitivity to the soil mechanical properties and use it to properly identify the susceptibility computational map.

The performance of the susceptibility maps, obtained by both the statistical analysis and TRIGRS, is evaluated considering two indicators: the area under curve, AUC, of the related receiver operating characteristic curve (ROC) (Metz, 1978), and the overestimation index, OI, defined as:

$$OI = \frac{A_{out}}{A_{stab}} \cdot 100 \quad (5)$$

$$OI(5^\circ) = \frac{A_{out}}{A_{stab(5^\circ)}} \cdot 100 \quad (6)$$

where: A_{out} is the area computed unstable located outside the observed triggering area; A_{stab} is the area not affected by instability; $A_{stab(5°)}$ is the area not affected by instability obtained excluding from the study area the zones with a slope gradient inferior or equal to 5°.

Concerning the AUC, a perfect model fitting would be characterised by an AUC value of 1 and a model not better than random would be characterised by an AUC value of 0.5. OI, originally defined "error index" by Sorbino et al. (2007, 2010), is proposed in order to individuate the "*overestimation"* area, intended here as the area computed as unstable by the model but not inventoried as area affected by landsliding.

3. Analyses and results

3.1. Statistical analyses

The variables employed within the statistical model have been expressed in raster format using 303071 square grid cells as TCUs, whose size is equal to 25 m^2. The dichotomous dependent variables, derived from two inventories of shallow landslides that occurred in 2009 and 2010, report 117 and 509 triggering areas which cover, respectively, 3421 and 10602 TCUs of the study area. The independent variables used in the analysis (Fig. 6, Table 1) are the five variables deemed to be

the most relevant following Calvello and Ciurleo (2016). The first three variables, i.e. elevation zone (V1), slope gradient (V2) and slope curvature (V3), are computed from the native-resolution variables, processing them by means of focal statistics techniques so that the information they carry is averaged over a larger area around them. The area of influence considered for the three variables depends on the diameter of the buffer considered around each TCU, herein called D_k, which is respectively equal to 32 cells for V1, and to 4 cells for V2 and V3. All three variables are classified according to a natural breaks criterion employing eight classes. The categorical variables outcropping lithology (V4) is divided in four classes; in this case, as already mentioned, the sandstone morphoselective scarp has been excluded from the analysis. The weathered rock thickness variable (V5) is divided in eight classes following the classification reported in the employed thematic map.

Table 2, reporting the values of the statistical weights computed using Eq. (1) for each class of each independent variable Vi, underlines that the maximum weights computed considering the dichotomous dependent variables, respectively dated 2009 and 2010, are both attributed to class 8 of variable V2 (W_{28}=1.28 in 2009 and W_{28}=1.15 in 2010). High values of weights are computed for variables V1, V3 and V5 both in 2009 and 2010: W_{18}(2009)=0.98; W_{18}(2010)=0.68; W_{31}(2009)=1.06; W_{31}(2010)=0.94; W_{52}(2009)=0.55; W_{52}(2010)=0.60. Out of the four classes of variable V4, only one geological unit, which is the class corresponding to silty clays with sporadic sand intercalations, assumes a positive weight value, W_{44}=0.28, for both years. Concerning low negative values of the weights, it is worth highlighting that only one class is characterised by a weight value equal to -2.59 (W_{23}), while the W_{ij} equal to -3.00 is imposed whenever the argument of the logarithm used in Eq. (1) is equal to zero (Ciurleo et al., 2016).

All the independent considered variables are relevant for the analysis as testified by the value of β_i (Eq. 2) and σ_i (Eq. 3) respectively greater than 1.7 and 0.4 (Ciurleo et al., 2016), as reported in Table 3. The Table also shows the values of the two statistics needed to compute the bivariate success index, TPR_i and FPR_i. Fig. 7 shows two landslide susceptibility computational maps classified on the basis of the values assumed by the multivariate computational susceptibility index, respectively considering the dichotomous dependent variables dated 2009 and 2010, IS_{TCU}, as follow: not susceptible, for $IS_{TCU} \leq 0$; susceptible for $IS_{TCU} > 0$. The results indicate that about 20% of the study area is susceptible (i.e. $IS_{TCU} > 0$) in 2009; this area increases to 24% in 2010. The success of the analysis is verified by the high value assumed by the area under curve (AUC) of the ROC curve plotted in the sensitivity versus (1 − specificity) space, with values ranging from 96% in 2009

to 95% in 2010. On the contrary, the values of OI and OI(5°) are never too low, as they range from OI=19% (in 2009) to OI=21% (in 2010) and OI(5°)=27% (in 2009) to OI(5°)=30% (in 2010).

3.2. Deterministic analyses

The input data employed within TRIGRS, as for the variables used in the statistical analyses, are expressed in raster format using 5×5 m^2 square grid cells as TCUs. The input data used in TRIGRS are the following: DEM, flow direction, thickness map, initial water table location, geotechnical properties of the soils and rainfall data.

Flow direction has been directly derived by DEM with single cell size equal to 5×5 m^2. Following Cascini et al. (2017) it was possible to both reconstruct the thickness map (Fig. 5b) and localize the initial water table at the contact between intact and weathered rocks.

Referring to the geotechnical properties, the study area is analysed following two different cases (Tab. 4): case 1, assigning the same geotechnical input data for the entire study area; case 2, differentiating the geotechnical properties in relation to the thickness of the weathered rock. In particular, for case 1 the assigned geotechnical parameters are equal to the minimum values available from the geotechnical input data. For case 2, different geotechnical properties are assumed for three classes of thickness (0.5-1.0 m; 1.0-2.0 m and 2.0-3.0 m) corresponding to three different shallow landslide mechanisms. These values have been provided by Cascini et al. (2017) who, by means of 2D geotechnical analyses, were able to back-analyse these shallow precipitation-induced landslides and to provide different values of cohesion and friction angle for which the factor of safety is equal to 1 along the assumed sliding surface. This is essentially due to the genesis of the landslide mechanisms and to their close relationship with the weathering processes (Cascini et al., 2017).

The obtained results (Fig. 8) are provided for both cases assuming a value of rainfall input data equal to 162 mm in six days (Cascini et al., 2017). The results clearly show a consistent decrease of the unstable areas passing from case 1 (minimum geotechnical data) to case 2 (different geotechnical data depending on the weathered thickness). This reduction appears evident also when comparing, using the indicators AUC, OI and OI(5°), the obtained results with the landslide inventories dated 2009 and 2010. For Case 1, the AUC values range from 92% to 91%, respectively computed considering the shallow landslide inventories dated 2009 and 2010; the OI values range from 18% (in 2009) to 16% (in 2010); the OI(5°) values range from 25% (in 2009) to 23 % (in 2010). For case 2, the obtained results show: AUC = 93%, OI = 9% and OI(5°)=13% for the

landslide inventory dated 2009; AUC= 92%, OI = 8% and OI(5°)=11% for the landslide inventory dated 2010. Comparing the results obtained from case 1 and case 2, it is evident that, despite the AUC value does not improve significantly, there is a significant reduction of the OI value, passing from 18% to 9% in 2009 and from 16% to 8% in 2010, and of the OI(5°) values, going from 25% to 13% (in 2009) and from 23% to 11% (in 2010).

4. Discussion and concluding remarks

The paper presented a comparison, within a study area located in southern Italy, between statistical and deterministic methods used as tools for shallow landslides susceptibility assessment in clayey soils. To this purpose, the information value method for the statistical analyses and TRIGRS for the deterministic analyses have been used at large scale (1:5000). The information value method has been implemented using two dichotomous dependent variables (landslide inventories, years 2009 and 2010); TRIGRS model has been applied referring to two different geotechnical datasets (case 1 and case 2). In total, we obtained four landslide computational maps that have been compared by means of three indicators: AUC of the ROC curves, OI and OI(5°).

The very high values attained by the AUC testify the success of all the performed analyses. Indeed, independently from the method and the reference landslide inventory used, AUC is always greater than 90%, with values ranging from 95-96% for the statistical analyses and 91-92% for the deterministic analyses. The 90% AUC value is defined by Swets (1988) and Fressard et al. (2014) as a threshold to overcome for reaching the best class of accuracy for a model being tested. In particular Swets (1988) states that values between about 0.7 and 0.9 represent accuracies that are useful for some purposes, and higher values represent a rather high accuracy; whereas Fressard et al. (2014) state that values between 0.7 and 0.8 reflect a fair performance of the model, values between 0.8 and 0.9 can be considered good, and values above 0.9 can be considered excellent. To stress the relevance of the results obtained in this case study it is important to highlight that, within the literature dealing with landslide susceptibility and hazard assessment, few analyses report AUC values higher than 85% (e.g., Akgun, 2012; Yesilnacara and Topalb, 2005; Lee and Pradhan, 2006; Blahut et al., 2010; Yeon et al., 2010; Sterlacchini et al., 2011; Das et al., 2012) and even fewer AUC values higher than 90% (e.g., Lee et al., 2008; Bui et al, 2012; Marjanović 2013; Nefeslioglu et al., 2008; Ciurleo et al., 2016).

The success of the analyses is also related to the values assumed by over-prediction indexes such as: the modified success rate, MSR (Huang and Kao, 2006); the false positive rate of the contingency

table (Godt et al., 2008; Montrasio et al., 2011; Raia et al., 2013; Ciurleo et al., 2016); the error index, EI (Sorbino et al., 2010); the landslide potential, LP (Vieira et al., 2010); and the false alarm ratio, FAR (Liao et al., 2011). Among them, we choose the EI index, originally proposed by Sorbino et al. (2007, 2010) and named OI in this paper, in order to quantify the overestimation areas. In the case study, the area computed as unstable by the statistical analyses is equal to 1.5 Km^2 (2009) and 1.8 Km^2 (2010), while unstable TRIGRS cells involve an area of 1.4 Km^2 (case 1) and 0.8 Km^2 (case 2). These values, if compared with the inventoried ones (0.1 Km^2 of triggering areas inventoried in 2009 and 0.2 Km^2 in 2010), show a clear over-prediction ratio. This overestimation, identified by means of OI and OI(5°), is more evident for the statistical analyses and progressively decrease, moving from case 1 to case 2, when using TRIGRS. In particular, the statistical OI values are equal to 19% in 2009 and 21% in 2010, while the TRIGRS OI values range from 16% to 18% for case 1 and from 8% to 9% for case 2. The difference in the OI values becomes more evident when comparing the lowermost statistical OI(5°) value, equal to 27% (considering the 2009 landslides) with the lowermost OI(5°) value for the analyses with TRIGRS, equal to 11% (for case 2 in 2010). To explain these findings, it is worthwhile highlighting herein that TRIGRS's case 1 refers to a simplified geotechnical scheme (low strength characteristics for the overall investigated area) while case 2 employs different geotechnical parameters in relation to different thicknesses of the weathered rock layer. In the latter case, very low values of both OI and OI(5°) testify that an exhaustive understanding of the main physical and mechanical characteristics of the analysed phenomena is extremely relevant for the application of a deterministic model. Finally, considering that the same common input data have been used (in terms of quality and accuracy) for the statistical and the deterministic analyses, it is reasonable to assume that the higher overestimation recorded by the statistical analyses is related to the inherent inability of statistical methods to consider the physical processes within the soils predisposing or triggering the landslides.

In conclusion, the analyses performed over the same study area, to evaluate both the potentialities of the adopted methods and the consistency of the obtained results, indicate that statistical and deterministic analyses can be confidently developed at large scale for shallow landslide susceptibility assessment. The main results indicate that the statistical method provides shallow landslide susceptibility maps that are more conservative than those obtained by the physically-based model TRIGRS. The reliability of this latter progressively increases when the predisposing and triggering factors of the studied phenomena are properly characterized and used as input data.

REFERENCES

Antronico, L., Borrelli, L., Coscarelli, R., Pasqua, A.A., Petrucci, O., Gulla`, G., 2013. Slope movements induced by rainfalls damaging an urban area: The Catanzaro case study (Calabria, southern Italy). Landslides 10, 801–814.

Akgun, 2012. A comparison of landslide susceptibility maps produced by logistic regression, multi-criteria decision, and likelihood ratio methods: a case study at İzmir, Turkey. Landslides 9, 93-106.

Armas, I., Stroia, F., Giurgea, L., 2013. Statistic Versus deterministic Method for Landslide Susceptibility Mapping. Margottini et al. (eds.), Landslide Science and Practice, Vol. 3, DOI 10.1007/978-3-642-31310-3_52.

Baeza, C., Corominas, J., 2001. Assessment of shallow landslide susceptibility by means of multivariate statistical techniques. Earth Surface Processes and Landforms, 26, 1251–1263.

Baum, R.L., Coe, J.A., Godt, J.W., Harp, E.L., Reid, M.E., Savage, W.Z., Schulz, W.H., Brien D.L., Chleborad, A.F., McKenna, J. P., Michael J.A., 2005. Regional landslide-hazard assessment for Seattle,Washington, USA. Landslides 2, 266–279.

Blahut., J., VanWesten, C., Sterlacchini, S., 2010. Analysis of landslide inventories for accurate prediction of debris-flow source areas. Geophys J Roy Astron Soc, 119, 36–51.

Borrelli, L., Cofone, G., Coscarelli, R., Gullà, G., 2015. Shallow landslides triggered by consecutive rainfall events at Catanzaro strait (Calabria-Southern Italy). J. Maps 11, 730–744.

Borrelli, L., Gioffrè, D., Gullà, G., Moraci, N., 2012. Susceptibility to shallow and rapid landslides in ground alteration: A possible contribution of propagation modeling. Rendiconti Online Società Geologica Italiana, 21, 534-536.

Broothaerts, N., Kissi, E., Poesen, J., Van Rompaey, A., Getahun, K., Van Ranst, E., Diels, J., 2012. Spatial patterns, causes and consequences of landslides in the Gilgel Gibe catchment, SW Ethiopia. Catena 97, 127–136.

Bui, D., Pradhan, B., Lofman, O., Dick, O., 2012. Landslide susceptibility assessment in the Hoa Binh Province of Vietnam: a comparison of the Levenberg-Marquardt and Bayesian regularized neural networks. Geophys J Roy Astron Soc., 171–172, 12–29.

Calvello, M., Ciurleo, M., 2016. Optimal use of thematic maps for landslide susceptibility assessment by means of statistical analyses: case study of shallow landslides in fine grained soils. Proc. ISL 2016, Landslides and Engineered Slopes. Experience – Theory and Practice, Napoli, Italy, Vol. 2, p.537-544, ISBN: 978-1-138-02988-0.

Calvello, M., Cascini, L., Mastroianni, S., 2013. Landslide zoning over large areas from a sample inventory by means of scale-dependent terrain units. Geomorphology 182, 33–48.

Carrara, A., 1983. A multivariate model for landslide hazard evaluation. Mathematical Geology 15, 403–426.

Cascini, L., 2008. Applicability of landslide susceptibility and hazard zoning at different scales. Eng. Geol. 102, 164–177.

Cascini, L., Ciurleo, M., Di Nocera, S., Gullà, G., 2015. A new–old approach for shallow landslide analysis and susceptibility zoning in fine-grained weathered soils of southern Italy. Geomorphology 241, 371–381.

Cascini, L., Ciurleo, M., Di Nocera, S., 2017. Soil depth reconstruction for the assessment of the susceptibility to shallow landslides in fine-grained slopes. Landslides 14, 459–471.

Cervi, F., Berti, M., Borgatti, L., Ronchetti, F., Manenti, F., Corsini, A., 2010. Comparing predictive capability of statistical and deterministic methods for landslide susceptibility mapping: a case study in the northern Apennines (Reggio Emilia Province, Italy). Landslides 7, 433–444.

Ciurleo, M., Calvello, M., Cascini, L., 2016. Susceptibility zoning of shallow landslides in fine grained soils by statistical methods. Catena 139, 250–264.

Conforti, M., Robustelli, G., Muto, F., Critelli, S., 2012. Application and validation of bivariate GIS-based landslide susceptibility assessment for the Vitravo river catchment (Calabria, south Italy). Nat Hazards 61, 127–141.

Das, I., Stein, A., Kerle, N., Dadhwal, V., 2012. Landslide susceptibility mapping along road corridors in the Indian Himalayas using Bayesian logistic regression models. Geophys J Roy Astron Soc. 179, 116–125.

Fell, R., Corominas, J., Bonnard, C., Cascini, L., Leroi, E., Savage,W.Z., on behalf of the JTC-1 Joint Technical Committee on Landslides and Engineered Slopes, 2008. Guidelines for landslide susceptibility, hazard and risk zoning for land-use planning. Eng. Geol. 102, 85–98.

Frattini, P., Crosta, G., Carrara, A., 2010. Techniques for evaluating the performance of landslide susceptibility models. Engineering Geology 111, 62–72.

Fressard, M., Thiery, Y., Maquaire, O., 2014.Which data for quantitative landslide susceptibility mapping at operational scale: Case study of the Pays d'Auge plateau hillslopes (Normandy, France). Nat. Hazards Earth Syst. Sci. 14, 569–588.

Godt, J. W., Baum, R. B., Savage, W. Z., Salciarini, D., Schulz, W. H., and Harp, E. L., 2008. Transient deterministic shallow landslide modeling: Requirements for susceptibility and hazard assessments in a GIS framework, Eng. Geol. 102, 214–226.

Gullà, G., Aceto, L., Niceforo, D., 2004. Geotechnical characterisation of fine-grained soils affected by soil slips. Proc. of the 9th International Symposium on Landslides, Rio de Janeiro, Brazil, pp. 663–668.

Gullà, G., Aceto, L., Critelli, S., Perri, F., 2008. Geotechnical and mineralogical characterization of fine grained soils affected by soil slips. Proc. of the 10th International Symposium on Landslides, Xi'an, China, pp. 373–379.

Hadmoko, D.S., Lavigne, F., Samodra, G., 2017. Application of a semiquantitative and GIS-based statistical model to landslide susceptibility zonation in Kayangan Catchment, Java, Indonesia. Nat Hazards. DOI 10.1007/s11069-017-2772-z.

Huang, J. C., Kao, S. J., 2006. Optimal estimator for assessing landslide model performance Hydrol. Earth Syst. Sci. 10, 957–965.

Hungr, O., Evans, S.G., Bovis, M.J., Hutchinson, J.N., 2001. A review of the classification of landslides of the flow type. Environmental and Engineering Geoscience 3, 221-238.

O. Hungr, S. Leroueil, L. Picarelli (2014). The Varnes classification of landslide types, an update. Landslides, 11: 167–194

Iovine, G.G.R., Greco, R., Gariano, S.L., Pellegrino, A.D., Terranova, O.G. 2014. Shallow-landslide susceptibility in the Costa Viola mountain ridge (southern Calabria, Italy) with considerations on the role of causal factors. Nat Hazards 73, 111–136.

Jenks, G. F., 1977. Optimal data classification for choropleth maps. Geography Department Occasional Paper No. 2 2, University of Kansas, Lawrence, KS, 1977.

Kavzoglu, T., Sahin, E.K., Colkesen, I., 2015. Selecting optimal conditioning factors in shallow translational landslide susceptibility mapping using genetic algorithm. Engineering Geology 192, 101–112.

Lee, J.H, and Park, H.J., 2016. Assessment of shallow landslide susceptibility using the transient infiltration flow model and GIS-based probabilistic approach. Landslides 13, 885–903.

Lee, S., Pradhan, B., 2006. Probabilistic landslide hazard and risk mapping on Penang Island, Malaysia. J Earth Syst Sci. 115, 661–672.

Lee, C., Huang, C., Lee, J., Pan, K., Lin, M., Dong, J., 2008. Statistical approach to storm event-induced landsliZ des susceptibility. Nat Hazards Earth Syst Sci. 8, 941–960.

Leventhal, A.R., Kotze, G.P., 2008. Landslide susceptibility and hazard mapping in Australia for land-use planning — with reference to challenges in metropolitan suburbia. Engineering Geology 102, 238–250.

Liao, Z., Hong, Y., Kirschbaum, D., Adler, R. F., Gourley, J. J., and Wooten, R., 2011. Evaluation of TRIGRS (transient rainfall infiltration and grid-based regional slope-stability analysis)'s predictive skill for hurricane-triggered landslides: a case study in Macon County, North Carolina, Nat. Hazards. 58, 325–339.

Marjanović, 2013. Comparing the performance of different landslide susceptibility models in ROC space. Landslide Science and Practice, Volume 1: Landslide inventory and susceptibility and hazard zoning, 579-584.

Martinović, K., Gavina, K., Reale, C., 2016. Development of a landslide susceptibility assessment for a rail network. Engineering Geology 215, 1–9.

McDougall, S., Hungr, O., 2004. A model for the analysis of rapid landslide run out motion across three dimensional terrain. Canadian Geotechnical Journal 41, 1084–1097.

Meisina, C., 2006. Characterisation of weathered clayey soils responsible for shallow landslides. Nat. Hazards Earth Syst. Sci. 6, 825–838.

Metz, C.E., 1978. Basic principles of ROC analysis. Semin. Nucl. Med. 8, 283–298.

Montgomery, D.R., Dietrich, W.E., 1994. A physically based model for the topographic control on shallow landsliding. Water Resour. Res. 30, 1153–1171.

Montrasio, L., Valentino, R., and Losi, G. L., 2011. Towards a real-time susceptibility assessment of rainfall-induced shallow landslides on a regional scale, Nat. Hazards Earth Syst. Sci. 11, 1927–1947, doi:10.5194/nhess-11-1927-2011.

Nandi, A., Shakoor, A., 2009. A GIS-based landslide susceptibility evaluation using bivariate and multivariate statistical analyses. Engineering Geology 110, 11–20.

Nefeslioglu, HA., Gokceoglu, C., Sonmezb, H., 2008. An assessment on the use of logistic regression and artificial neural networks with different sampling strategies for the preparation of landslide susceptibility maps. Eng. Geol. 97, 171–191.

Park, H.J., Lee, J.H., Woo, I, 2013. Assessment of rainfall-induced shallow landslide susceptibility using a GIS-based probabilistic approach. Engineering Geology 161, 1–15.

Raia, S., Alvioli, M., Rossi, M., Baum, R. L., Godt, J. W., and Guzzetti, F., 2013. Improving predictive power of physically based rainfall-induced shallow landslide models: a probabilistic approach, Geosci. Model Dev. Discuss., 6, 1367–1426, doi:10.5194/gmdd-6-1367-2013.

Regmi, N.R., Giardino, J.R., McDonald, E.V., Vitek, J.D., 2014. A comparison of logistic regression-based models of susceptibility to landslides in western Colorado, USA. Landslides 11, 247–262.

Reza, M., Daneshvar, M., 2014. Landslide susceptibility zonation using analytical hierarchy process and GIS for the Bojnurd region, northeast of Iran. Landslides 11, 1079–1091.

Romer, C., Ferentinou, M., 2016. Shallow landslide susceptibility assessment in a semiarid environment — A Quaternary catchment of KwaZulu-Natal, South Africa. Engineering Geology 201, 29–44.

Salciarini, D, Godt, J.W., Savage, W.Z., 2006. Modeling regional initiation of rainfall-induced shallow landslides in the eastern Umbria Region of central Italy. Landslides 3, 181–194.

Soeters, R., van Westen, C.J., 1996. Slope instability recognition, analysis and zonation. In: Turner, A.K., Schuster, R.L. (Eds.), Landslides Investigation and Mitigation. TRB Special Report 247. National Academy Press, Washington D.C., pp. 129–177.

Sorbino, G., Sica, C., Cascini, L., Cuomo, S., 2007. On the forecasting of flowslides triggering areas using physically based models. Proceedings of 1st North American Landslides Conference, AEG Special Publication. 23, pp. 305–315.

Sorbino, G., Sica, C., Cascini, L., 2010. Susceptibility analysis of shallow landslides source areas using physically based models. Nat. Hazards 53, 313–332.

Srivastava, R., Yeh, T.-C. J., 1991. Analytical solutions for one-dimensional, transient infiltration toward the water table in homogeneous and layered soils: Water Resources Research v. 27, pp. 753–762.

Sterlacchini, S., Ballabio, C., Blahut, J., Masetti, M., Sorichetta, A., 2011. Spatial agreement of predicted patterns in landslide susceptibility maps. Geophys J Roy Astron Soc. 125, 51–61

Swets, J.A., 1988. Measuring the accuracy of diagnostic systems. Science 240, 1285–1293.

Tangestani, M.H., 2009. A comparative study of Dempster-Shafer and fuzzy models for landslide susceptibility mapping using a GIS: an experience from Zagros Mountains, SW Iran. J. Asian Earth Sci. 35, 66–73.

Taylor, DW, 1948. Fundamentals of soil mechanics. Wiley, New York, 700 p.

Vieira, B.C., Fernandes, N.F., Filho, O.A., 2010. Shallow landslide prediction in the Serra do Mar, São Paulo, Brazil, Nat. Hazards Earth Syst. Sci., 10, 1829–1837, doi:10.5194/nhess-10-1829-2010.

Wu, W., Sidle, RC., 1995. A distributed slope stability model for steep forested basins. Water Resour Res 31, 2097–2110.

Yeon, Y., Han, J., Ryu, K., 2010. Landslide susceptibility mapping in Injae, Korea using a decision tree. Eng Geol. 166, 274–28.

Yerro, A., Alonso, E.E., Pinyol, N.M., 2016. Run-out of landslides in brittle soils. Computers and Geotechnics 80, 427–439.

Yesilnacara, E., Topalb, T., 2005. Landslide susceptibility mapping: A comparison of logistic regression and neural networks methods in a medium scale study, Hendek region (Turkey). Eng Geol. 79, 251–266.

Yin, K.J., Yan, T.Z., 1988. Statistical prediction model for slope instability of metamorphosed rock. Proc. 5th Int.l Symposium on Landslides, Lausanne, Switzerland vol. 2l, pp. 1269–1272.

Tab.1. Classification of the independent variables employed in the statistical analysis at large scale.

Class	V1 elevation zone (m)	V2 slope gradient (°)	V3 slope curvature (m− 1)	V4 geological unit (−)	V5 weathered thickness (−)
1	30.39 to 55.86	0.00 to 4.12	− 6.12 to − 2.06	Colluvial deposits	0.00–0.50
2	55.87 to 81.33	4.13 to 8.59	− 2.05 to − 1.02	Halluvial deposits	0.50–1.00
3	81.34 to 105.98	8.60 to 12.89	− 1.01 to − 0.36	Slope debris	1.00–1.50
4	105.99 to 130.63	12.90 to 17.00	− 0.35 to 0.13	Silty clays with sporadic sand intercalation	1.50–2.00
5	130.64 to 154.46	17.01 to 20.94	0.14 to 0.74		2.00–3.00
6	154.47 to 178.29	20.95 to 25.06	0.75 to 1.56		3.00–4.00
7	178.30 to 230.76	25.07 to 30.07	1.57 to 2.71		4.00–5.00
8	230.77 to 239.91	30.07 to 45.64	2.72 to 7.87		> 5.00

Tab.2. Weights assigned to the independent variables in the statistical analysis at large scale.

Weights 2009	V1	V2	V3	V4	V5	Weights 2010	V1	V2	V3	V4	V5
Wi1	− 3.00	− 3.00	1.06	− 3.00	− 0.26	Wi1	− 3.00	− 3.00	0.94	− 3.00	− 0.26
Wi2	− 3.00	− 3.00	0.55	− 1.24	0.55	Wi2	− 3.00	− 3.00	0.50	− 1.38	0.60
Wi3	− 3.00	− 3.00	0.04	− 0.40	0.27	Wi3	− 3.00	− 2.59	0.05	− 0.43	0.17
Wi4	− 3.00	− 1.52	− 0.55	0.28	− 0.10	Wi4	− 1.29	− 1.26	− 0.52	0.28	− 0.17
Wi5	− 0.46	− 0.52	− 0.11		− 0.80	Wi5	0.07	− 0.22	− 0.13		− 0.52
Wi6	0.25	0.23	0.13		− 3.00	Wi6	0.42	0.36	0.22		− 1.42
Wi7	0.63	0.92	0.23		− 3.00	Wi7	0.66	0.89	0.40		− 3.00
Wi8	0.98	1.28	0.25		− 3.00	Wi8	0.68	1.15	0.48		− 3.00

Tab.3. Values of parameters and indexes needed to select the independent variables relevant for the statistical analysis at large scale.

Variables	2009				2010				
	TPR_i	FPR_i	β	σ_i	TPR_i	FPR_i	β	σ_i	Relevant
V1	95.8%	22.0%	4.36	2.20	99.3%	32.5%	3.05	2.17	Yes
V2	95.7%	17.6%	5.45	2.45	91.3%	15.8%	5.78	2.45	Yes
V3	73.3%	34.6%	2.12	0.77	72.9%	33.7%	2.17	0.74	Yes
V4	93.2%	48.8%	1.91	0.85	93.9%	47.7%	1.97	0.86	Yes
V5	84.0%	31.0%	2.71	2.23	84.0%	29.7%	2.83	2.22	Yes

Tab.4. The geotechnical input data used for TRIGRS analyses.

TRIGRS – Case 1					
Unit weight γ (kN/m3)	Effective cohesion c′ (kPa)	Friction angle ϕ′ (°)	Soil depth h TRIGRS (m)	Hydraulic conductivity K (m/s)	Diffusivity D TRIGRS (m2/s)
18	3	27	variable	5.00E – 06	2.87–05
TRIGRS – Case 2					
Unit weight γ (kN/m3)	Effective cohesion c′ (kPa)	Friction angle ϕ′ (°)	Soil depth h TRIGRS (m)	Hydraulic conductivity K (m/s)	Diffusivity D TRIGRS (m2/s)
18	3	27	0.5–1.0	5.00E – 06	2.87E – 05
18	5	27	1.0–2.0	5.00E – 07	3.49E – 05
18	8	27	2.0–3.0	5.00E – 07	3.49E – 05

Fig.1. Geographical location of the study area. Legend: 1. Pliocene light blue-grey silty clays; 2. zones frequently involved by shallow landslides studied in the past (S2 and S3); 3. study area (S1).

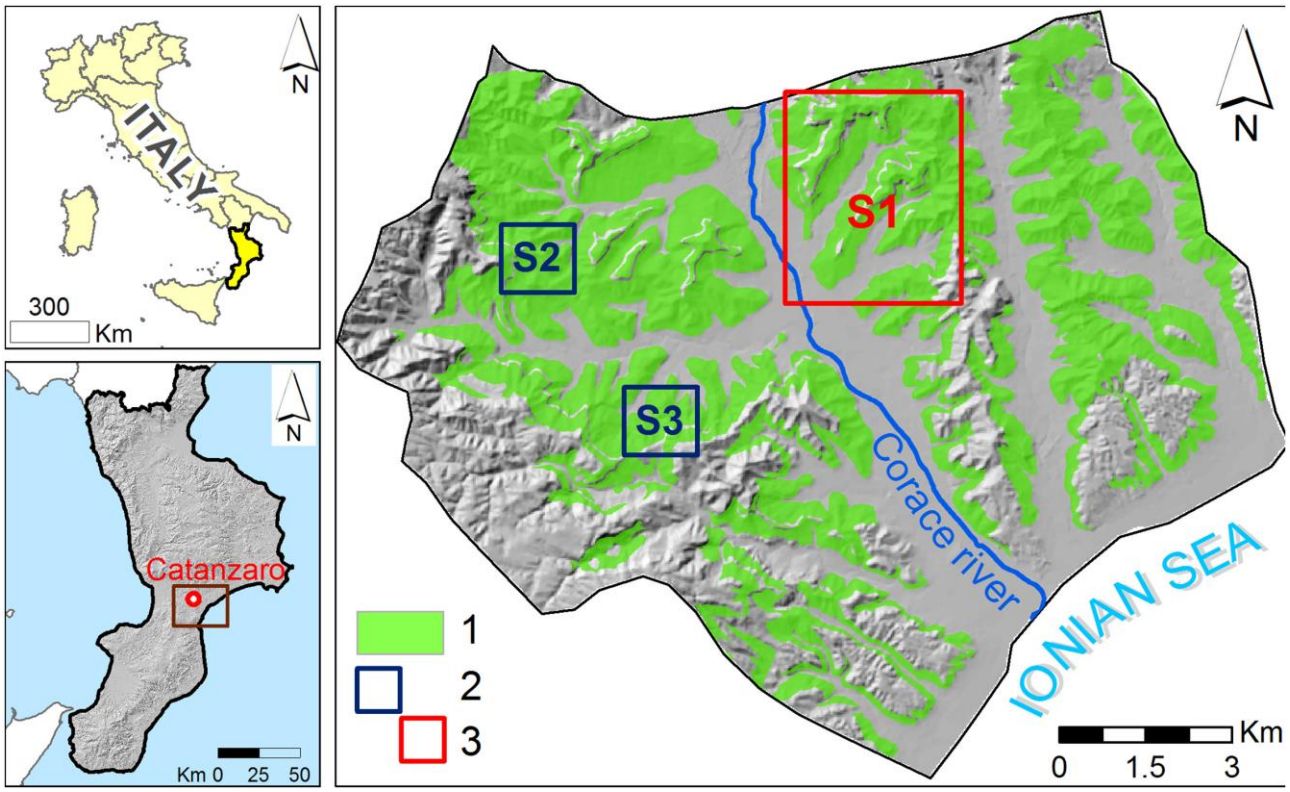

Fig. 2. Available in situ investigations and laboratory tests (modified from Cascini et al., 2017). a) Spatial location. b) Physical and mechanical properties of weathered clays. From the top to the bottom: plasticity chart, grain size distribution envelope, index properties (dry unit weight - γd (kN/m3), natural unit weight - γ (kN/m3), the saturated unit weight - γs (kN/m3), index void - e (−), soil porosity - n (−)), shear strength (modified from Gullà et al. 2008; Cascini et al. 2015).

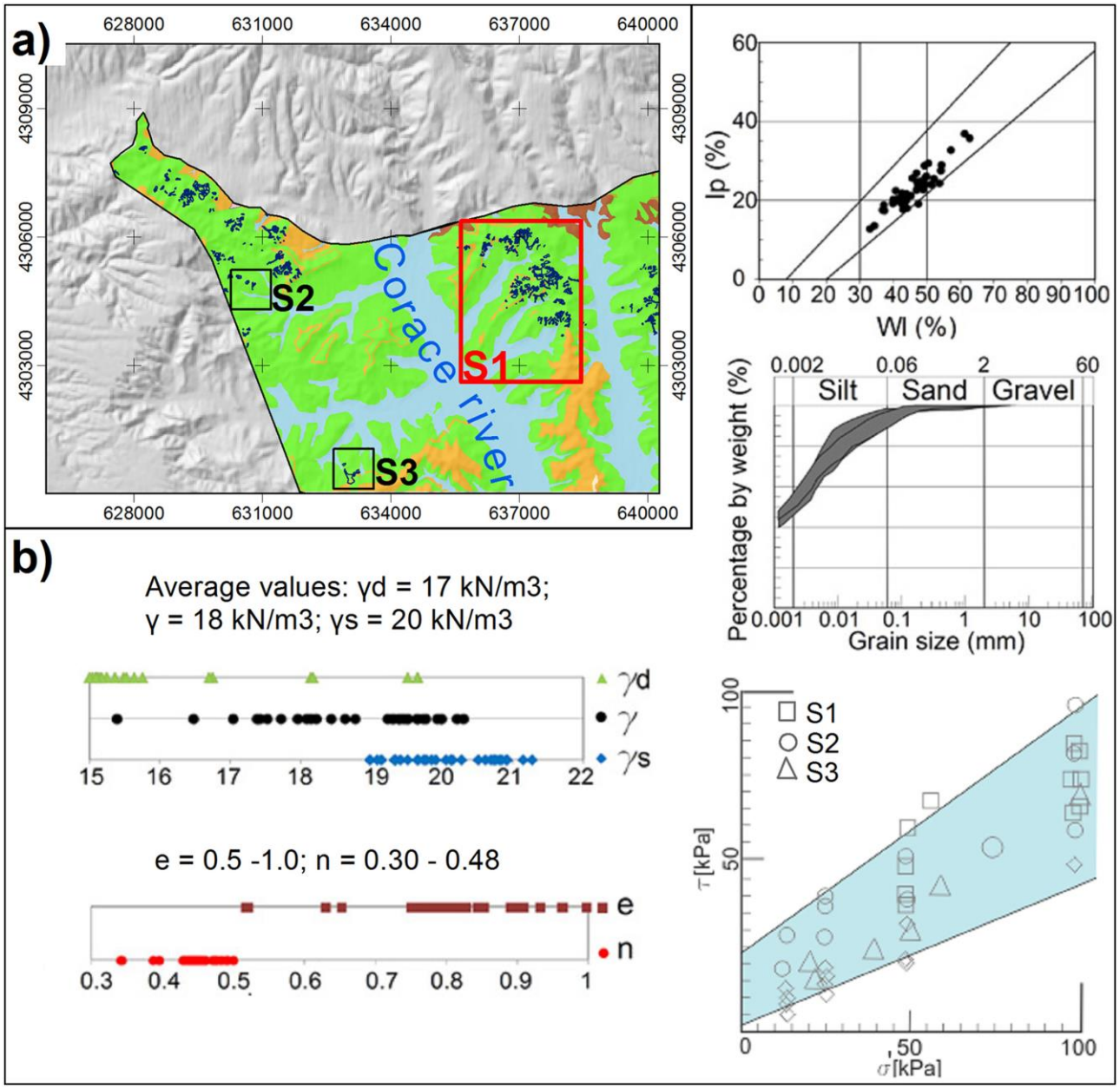

Fig. 3. Lithological map of the study area (S1), Legend: 1. alluvial deposits; 2. colluvial; 3. landslide debris; 4. light blue-grey silty clays; 5. Sandstone.

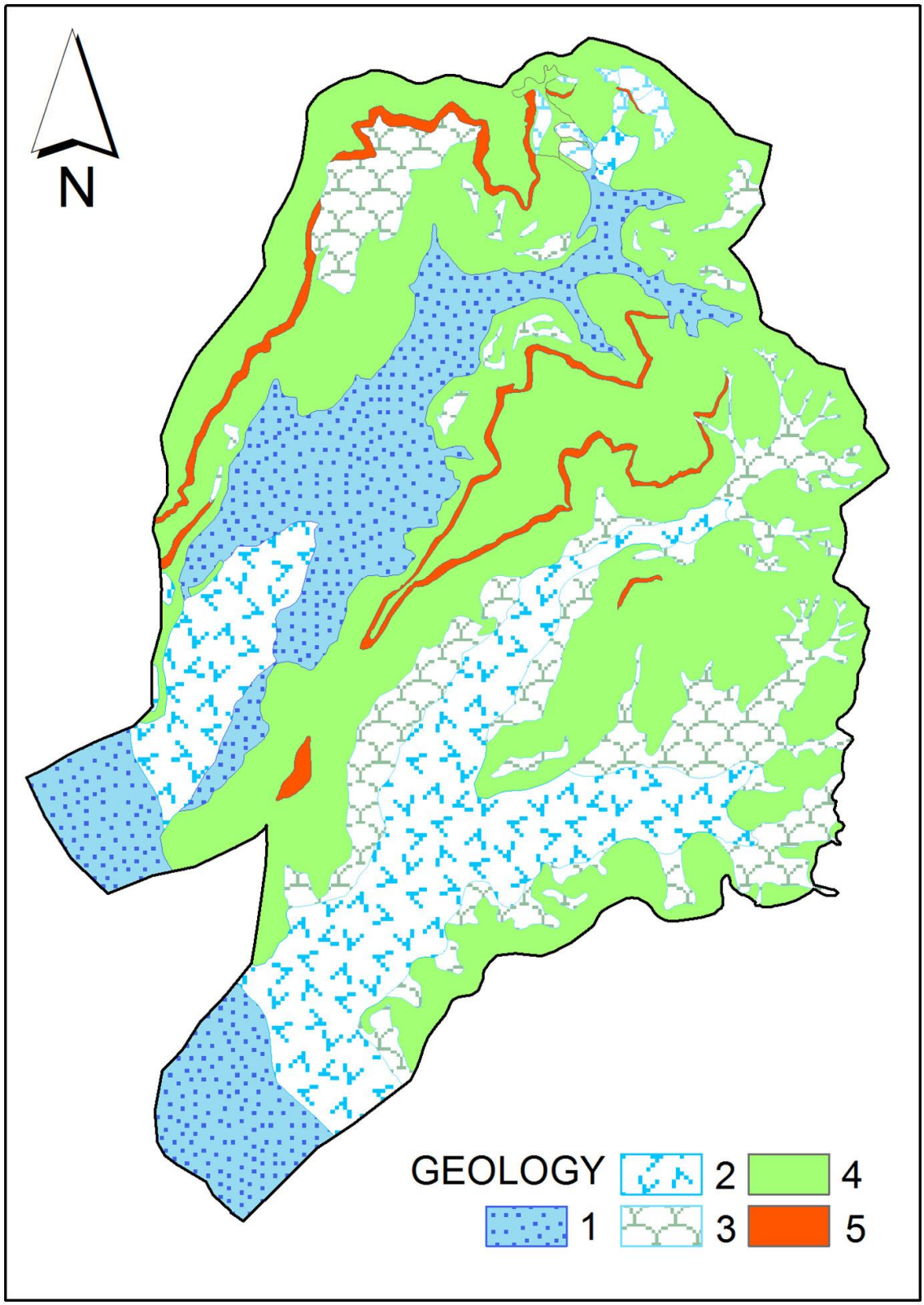

Fig. 4. 3D view from Google Earth of December 2005, April 2009 and March 2010 for the study area (S1).

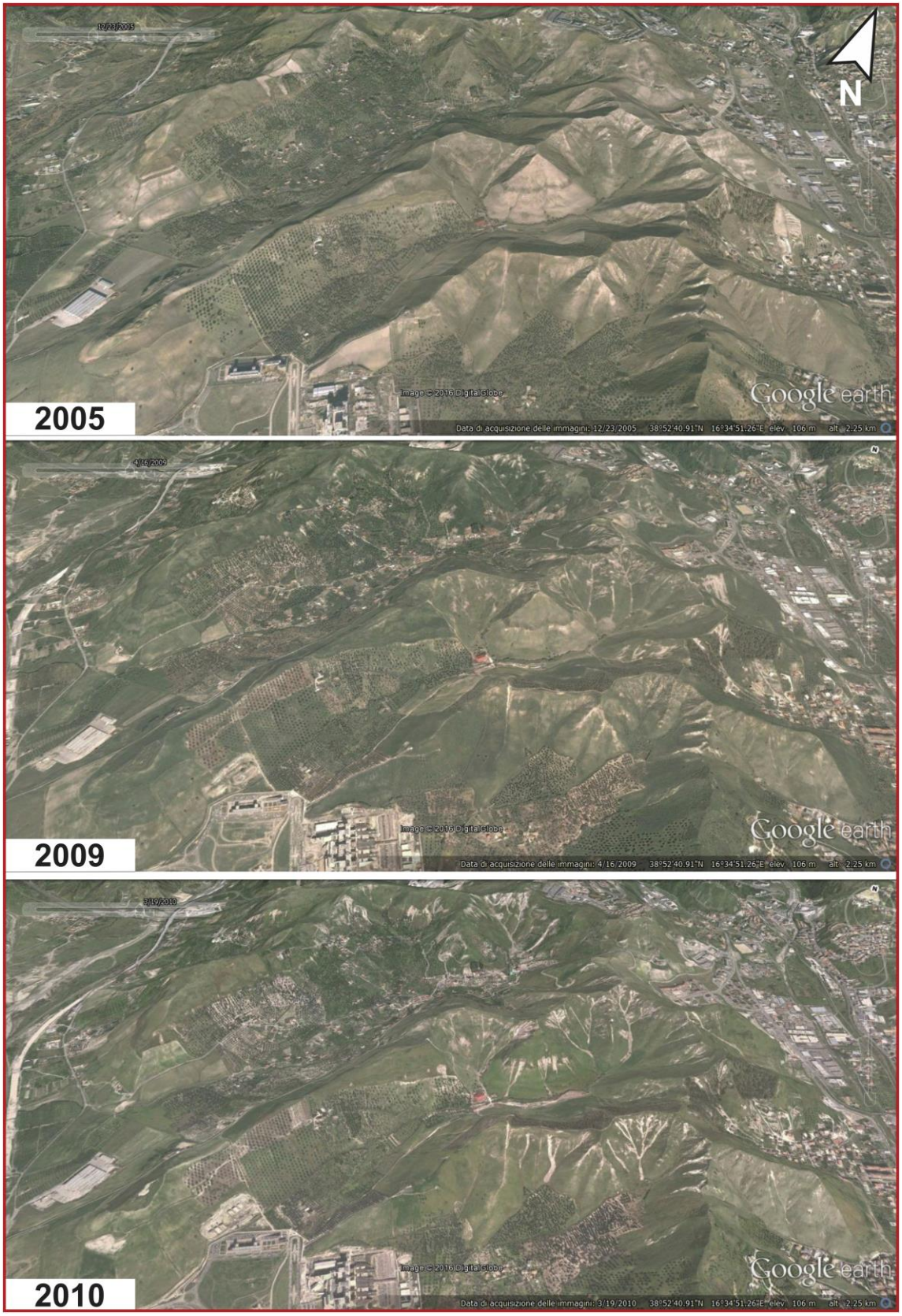

Fig. 5. Thematic map employed for the analysis at S1: a) Landslide inventories. Legend: landslide source areas from 2009 (1) and 2010 (2) inventories; b) Weathered rock thickness map.

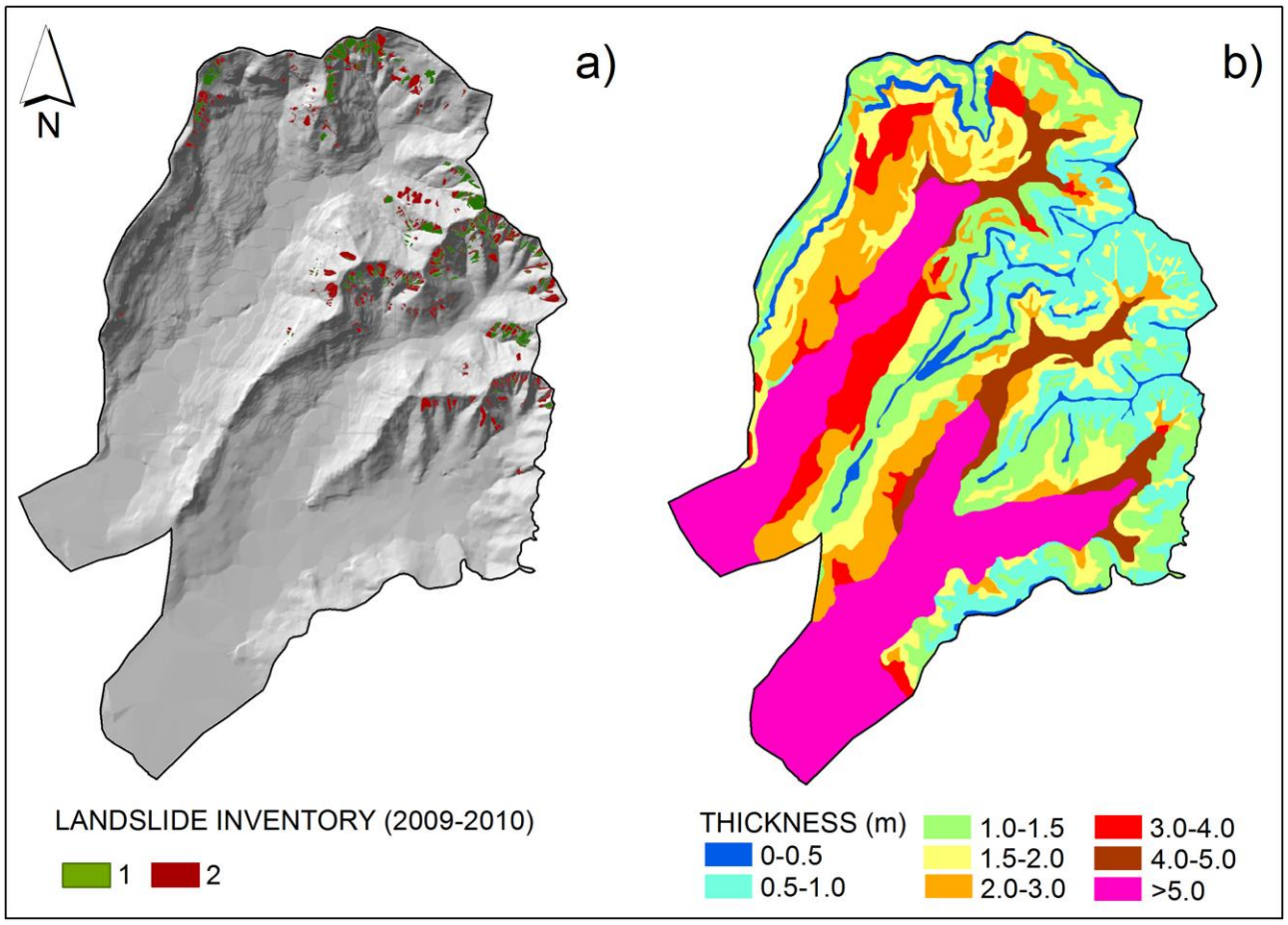

Fig. 6. Variables employed in the statistical analysis. Independent variables: (a) elevation zones, V1; (b) slope gradient, V2; (c) slope curvature, V3; (d) geology V4;(e) weathered rock thickness, V5. Dependent variables: (f) landslide source areas from 2009; g) landslide source areas from 2010. Legend for (d): 1. alluvial deposits; 2. colluvial; 3. slope debris; 4. light blue-grey silty clays.

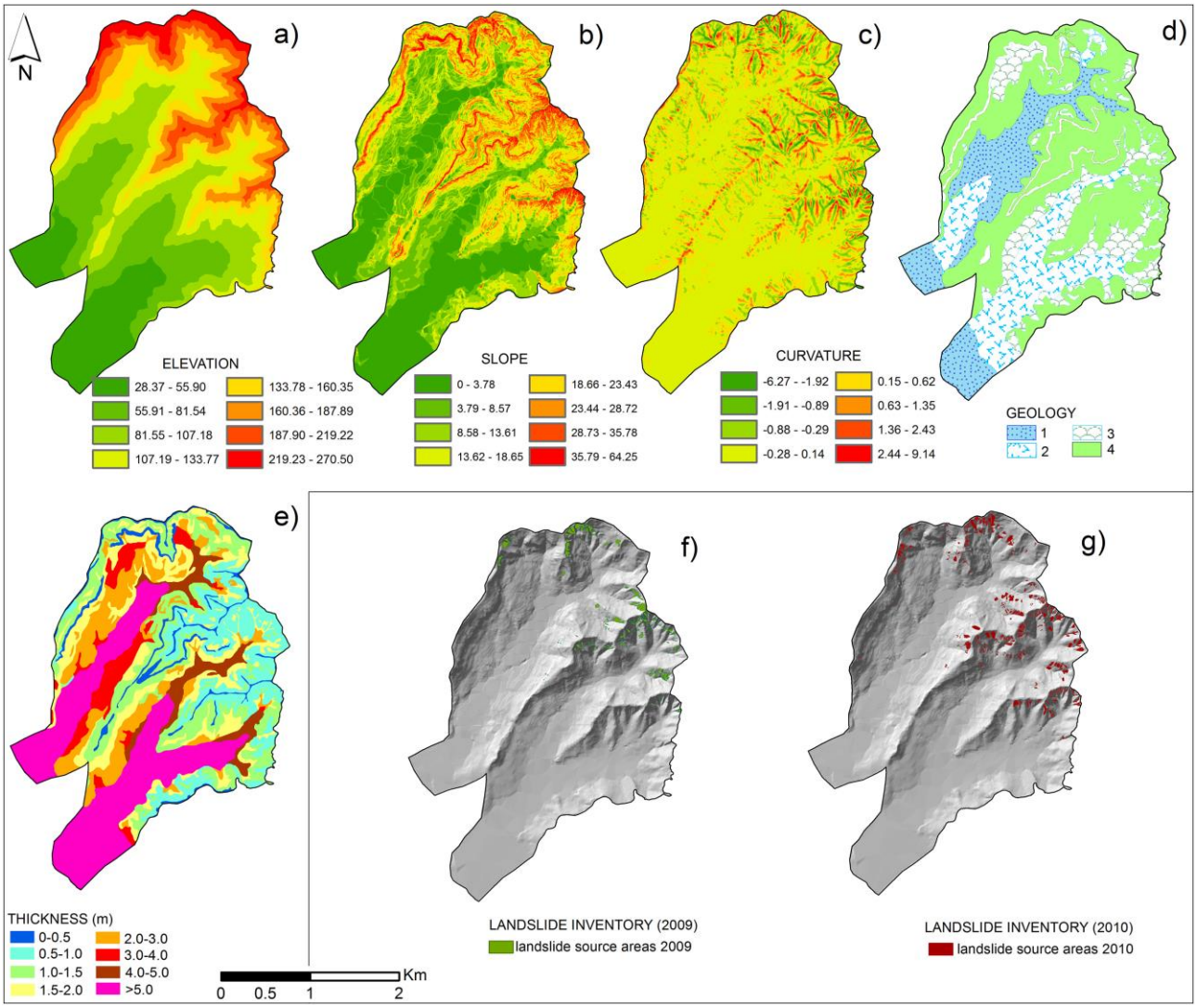

Fig. 7. Results of the statistical analyses at 2009 and 2010: landslide susceptibility computational maps; receiver operating characteristic curves; values of statistical indicators of performance AUC, OI and OI(5°).

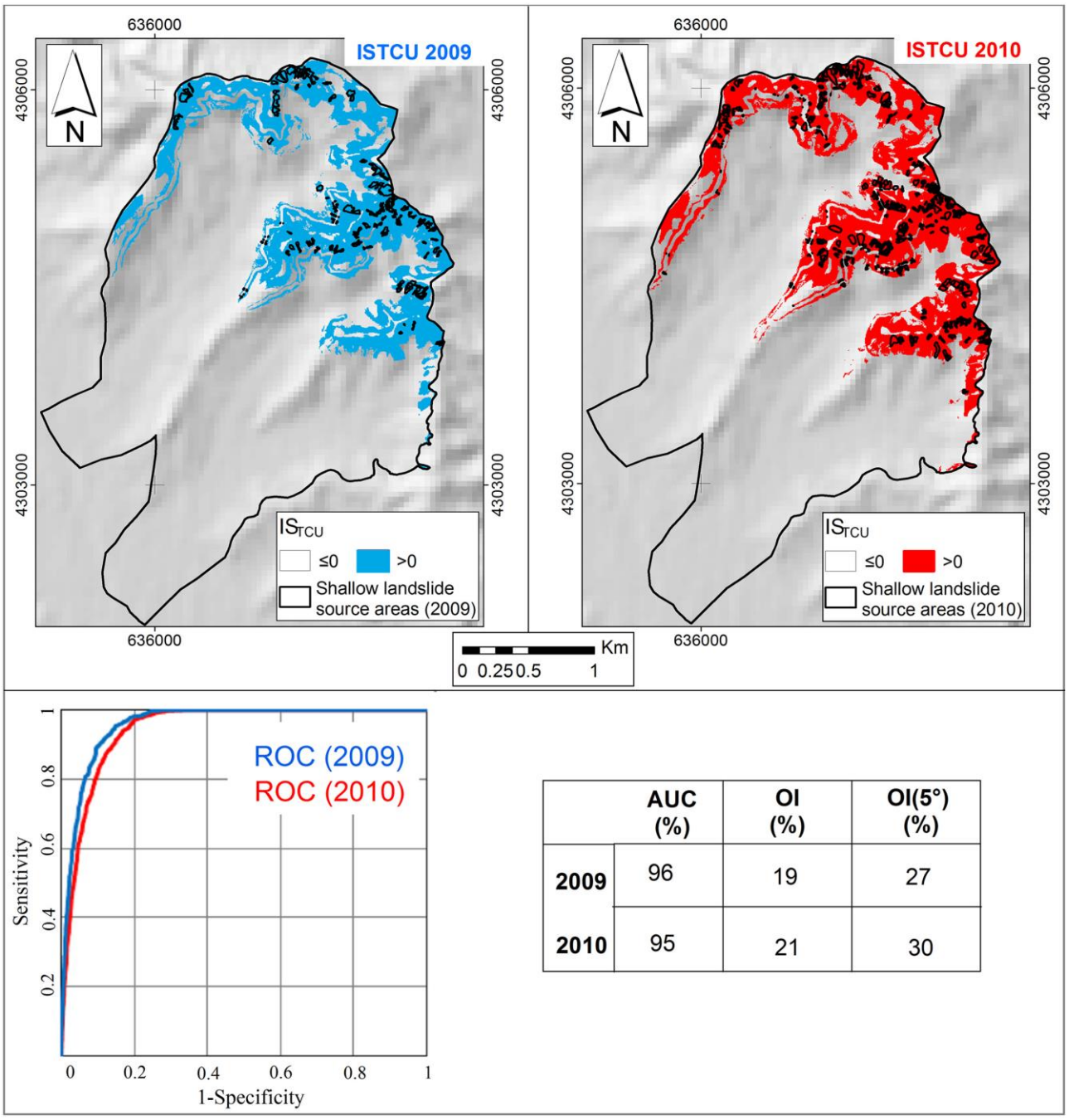

	AUC (%)	OI (%)	OI(5°) (%)
2009	96	19	27
2010	95	21	30

Fig. 8. Results of the TRIGRS analyses at 2009 and 2010 for case 1 and case 2: landslide susceptibility computational maps; receiver operating characteristic curves; values of statistical indicators of performance AUC, OI and OI(5°).

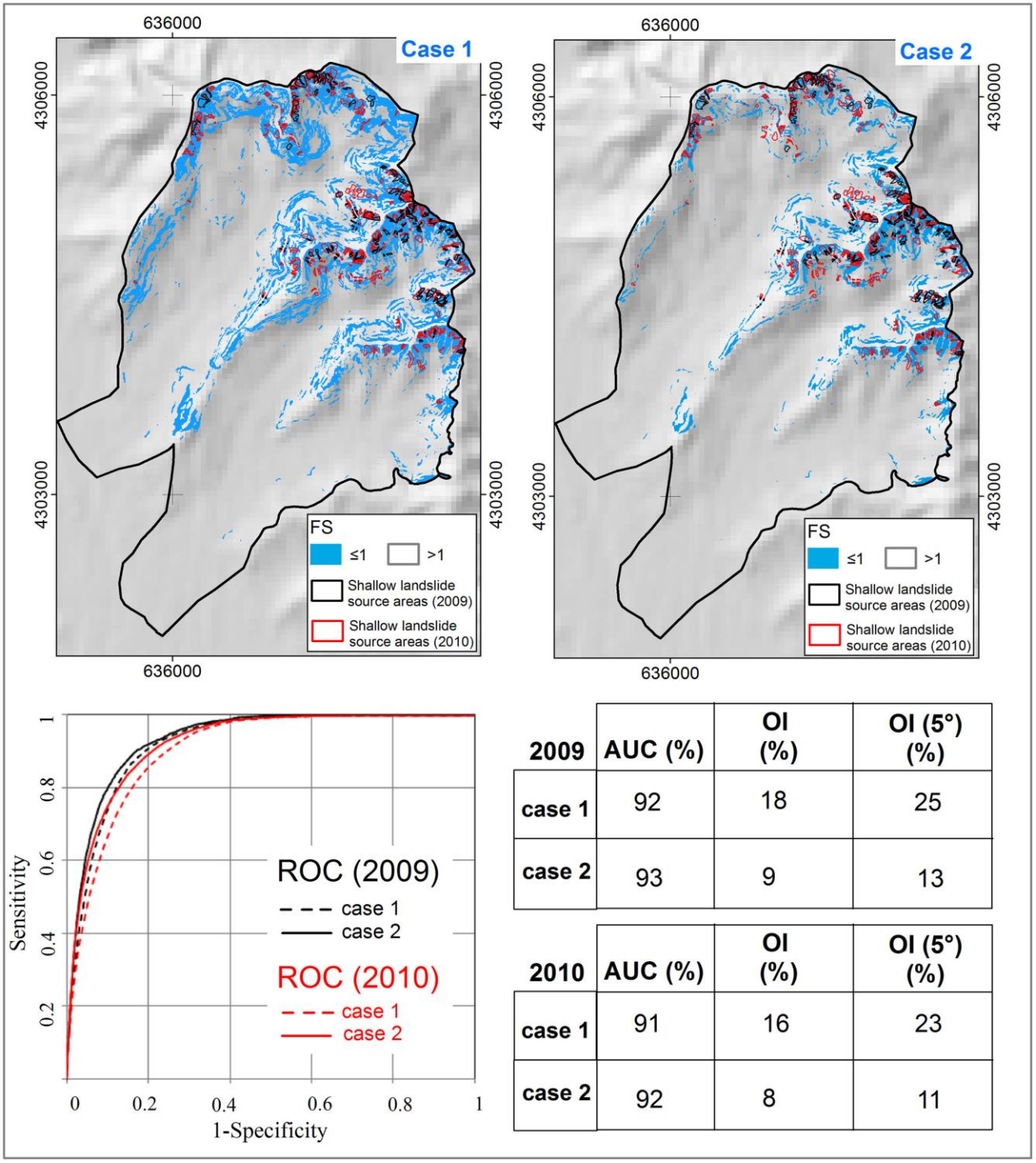

2009	AUC (%)	OI (%)	OI (5°) (%)
case 1	92	18	25
case 2	93	9	13

2010	AUC (%)	OI (%)	OI (5°) (%)
case 1	91	16	23
case 2	92	8	11